5566 *Chem. Mater.* **2009,** *21,* 5566–5568
DOI:10.1021/cm902745a

CHEMISTRY OF MATERIALS
Communication

Topotactic Li Insertion/Extraction in Hexagonal Vanadium Monophosphide

Cheol-Min Park,[†,§] Young-Ugk Kim,[‡] and Hun-Joon Sohn*[,†]

[†]*Department of Materials Science and Engineering, Research Center for Energy Conversion and Storage, Seoul National University, Seoul 151-742, Korea and* [‡]*Development Team, Battery Business Division, Samsung SDI, Seongseong-dong, Cheonan-si, Chungcheongnam-do 330-300, Korea.* [§]*Present address: Environmental Energy Technologies Division, Lawrence Berkeley National Laboratory, Berkeley, CA 94720*

Received September 2, 2009
Revised Manuscript Received October 29, 2009

There is active research into new materials or concepts for Li-ion batteries in order to enhance their electrochemical characteristics for applications to various portable electronics and hybrid electric vehicles (HEVs). In particular, to meet the need for longer-lasting electronic mobile devices and HEVs, researchers have devoted considerable work to improving the electrochemical properties of Li-ion battery anodes to replace the graphite anode currently in use.[1−3] Although the graphite anode has an interesting layered crystalline structure, which allows the intercalation reaction of Li, it has small capacity (372 mA h g^{-1}). Intercalation of Li into layered graphite suggests the stepwise formation of periodic Li arrays in the unoccupied graphene layer gaps, which requires energy to expand the van der Waals gap between two graphene layers and the repulsive interactions between Li ions.[3−5] These structural features contribute to negligible volume expansion during Li insertion/extraction, which results in excellent electrochemical behaviors of the graphite anode. Therefore, new higher capacity materials with similar intercalation concepts are required as alternative anodes for rechargeable Li-ion batteries.

Besides intercalation in graphite, Souza et al. suggested a new concept of a topotactic-intercalation mechanism, in which lithium is inserted into the monoclinic binary MnP_4 phase to form a cubic ternary Li_7MnP_4 phase.[6] Also, Doublet et al. reported the topotactic-intercalation on Li_xVPn_4 compounds.[7] Since then, Li insertion/extraction in P-based intermetallic or composite materials, such as ZnP_2,[8,9] VP_4,[10] NiP_2,[11,12] FeP_2,[13,14] CuP_2,[15] Cu_3P,[16] Sn_4P_3,[17−20] InP,[21] GaP,[21] CoP_3,[22,23] TiP_2,[24] black P,[25] and their nanocomposites[8,25] has been investigated as possible candidates as anode materials in Li-ion batteries. Recently, our group suggested a new concept of quasi-intercalation in layered materials (black P, gray As, and orthorhombic ZnSb),[25,26] in which a layered structure transformed into another layered structure of host atoms and periodic Li arrays through electrochemical recrystallization upon lithiation. Although the materials using topotactic- or quasi-intercalation concepts showed excellent electrochemical behavior, the materials have disadvantages in that the host structure is destroyed by successive cycling or should be used within controlled voltage windows.

Among the many binary phosphides, VP has a unique NiAs-type hexagonal structure. Although many phosphides are semiconductors and unstable at high temperatures, VP is a metallic conductor and quite stable up to at least 1050 °C.[27] Therefore, stable P-based electrodes can be achieved if VP can be used as an electrode material in Li-ion batteries.

This paper reports a new anode material of vanadium monophosphide (VP) for topotactic Li insertion/extraction. A hexagonal VP was synthesized by simple

*To whom correspondence should be addressed. E-mail: hjsohn@snu.ac.kr Tel: +82-2-880-7226. Fax: +82-2-885-9671.

(1) Nazri, G.-A.; Pistoia, G. *Lithium Batteries: Science and Technology*; Kluwer Academic/Plenum: Boston, 2004.
(2) Dahn, J. R.; Zheng, T.; Liu, Y.; Xue, J. S. *Science* **1995**, *270*, 590.
(3) Winter, M.; Besenhard, J. O.; Spahr, M. E.; Novak, P. *Adv. Mater.* **1998**, *10*, 725.
(4) Whittingham, M. S.; Jacobson, A. J. *Intercalation Chemistry*; Academic: New York 1982.
(5) Dresselhaus, M. S. *Intercalation in Layered Materials*; Plenum: New York 1986.
(6) Souza, D. C. S.; Pralong, V.; Jacobson, A. J.; Nazar, L. F. *Science* **2002**, *296*, 2012.
(7) Doublet, M.-L.; Lemoigno, F.; Gillot, F.; Monconduit, L. *Chem. Mater.* **2002**, *14*, 4126.
(8) Park, C.-M.; Sohn, H.-J. *Chem. Mater.* **2008**, *20*, 6319.
(9) Hwang, H.; Kim, M. G.; Kim, Y.; Martin, S. W.; Cho, J. *J. Mater. Chem.* **2007**, *17*, 3161.
(10) Kim, Y.-U.; Cho, B. W.; Sohn, H.-J. *J. Electrochem. Soc.* **2005**, *152*, A1475.
(11) Gillot, F.; Boyanov, S.; Dupont, L.; Doublte, M.-L.; Morcrette, M.; Monconduit, L.; Tarascon, J.-M. *Chem. Mater.* **2005**, *17*, 6327.
(12) Boyanov, S.; Bernardi, J.; Bekaert, E.; Menetrier, M.; Doublet, M.-L.; Monconduit, L. *Chem. Mater.* **2009**, *21*, 298.
(13) Silva, D. C. C.; Crosnier, O.; Ouvrard, G.; Greedan, J.; Safa-Sefat, A. *Electrochem. Solid-State Lett.* **2002**, *5*, A213.
(14) Boyanov, S.; Bernardi, J.; Gillot, F.; Dupont, L.; Womes, M.; Tarascon, J.-M.; Monconduit, L.; Doublet, M.-L. *Chem. Mater.* **2006**, *18*, 3531.
(15) Wang, K.; Yang, J.; Xie, J.; Wang, B.; Wen, Z. *Electrochem. Commun.* **2003**, *5*, 480.
(16) Bichat, M. P.; Politova, T.; Pascal, L.; Favier, F.; Monconduit, L. *J. Electrochem. Soc.* **2004**, *151*, A2074.
(17) Kim, Y.-U.; Lee, C. K.; Sohn, H.-J.; Kang, T. *J. Electrochem. Soc.* **2004**, *151*, A933.
(18) Leon, B.; Corredor, J. I.; Tirado, J. L.; Perez-Vicente, C. *J. Electrochem. Soc.* **2006**, *153*, A1829.
(19) Kim, Y.; Hwang, H.; Yoon, C. S.; Kim, M. G.; Cho, J. *Adv. Mater.* **2007**, *19*, 92.
(20) Wu, J.-J.; Fu, Z.-W. *J. Electrochem. Soc.* **2009**, *156*, A22.
(21) Satya Kishore, M. V. V. M.; Varadaraju, U. V. *J. Power Sources* **2006**, *156*, 594.
(22) Pralong, V.; Souza, D. C. S.; Leung, K. T.; Nazar, L. F. *Electrochem. Commun.* **2002**, *4*, 516.
(23) Alcantara, R.; Tirado, J. L.; Jumas, J. C.; Monconduit, L.; Olivier-Fourcade, J. *J. Power Sources* **2002**, *109*, 308.
(24) DeMattei, R. C.; Watcharapasorn, A.; Feigelson, R. S. *J. Electrochem. Soc.* **2001**, *148*, D109.
(25) Park, C.-M.; Sohn, H.-J. *Adv. Mater.* **2007**, *19*, 2465.
(26) Park, C.-M.; Sohn, H.-J. Adv. Mater. **2009**, DOI: 10.1002/adma.200901472.
(27) Corbridge, D. E. C. *Phosphorus: An Outline of its Chemistry, Biochemistry and Technology*, 5th ed.; Elsevier: Amsterdam, 1995.

 Published on Web 11/04/2009

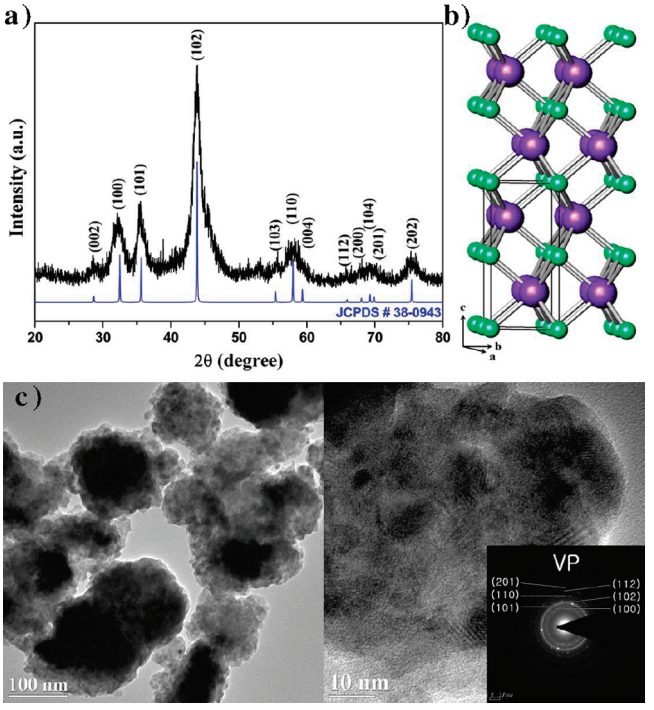

Figure 1. XRD patterns, crystal structure, and HRTEM image of VP: (a) XRD pattern of VP prepared by HEMM. (b) Crystal structure of hexagonal VP (V atoms, green; P atoms, purple). (c) TEM bright-field and HRTEM images.

high-energy mechanical milling (HEMM) at ambient temperature and pressure using amorphous red phosphorus and vanadium powder. Originally, hexagonal VP was prepared at high pressures and temperatures.[27] The temperature during HEMM can rise to more than 200 °C and that the pressure generated can be in the order of 6 GPa,[28] which are sufficient to transform red P and V into an alloying phase, hexagonal VP. This study examined the topotactic reaction mechanism and the electrochemical performance of the hexagonal VP electrode as an anode material in Li-ion batteries.

The VP powder was prepared using V (Kojundo, average size: 100 μm) and red P (Aldrich, average size: 15 μm) powders with HEMM (Spex-8000) at ambient temperatures and pressures. V and P powders were placed into a 80 cm^3 hardened steel vial with stainless steel balls (diameter: 3/8 in. and 3/16 in.) at a ball-to-powder ratio of 20:1. The HEMM process was carried out under an Ar atmosphere for 6 h. Figure 1a shows the X-ray diffraction (XRD, Rigaku, D-MAX2500-PC) patterns of hexagonal VP. The average crystallite size of the VP estimated from Scherrer's equation was approximately 15 nm. As shown in Figure 1b, VP has an interesting NiAs-type hexagonal crystalline structure ($P6_3/mmc$), which is composed of *a*-axis channels for facile Li diffusion and accommodation. Transmission electron microscopy (TEM, FEI F20, operating at 200 kV) bright-field and high-resolution TEM (HRTEM) combined with selected-area electron diffraction revealed well developed, crystalline VP nanoparticles consisting of aggregated ca.10−20 nm sized

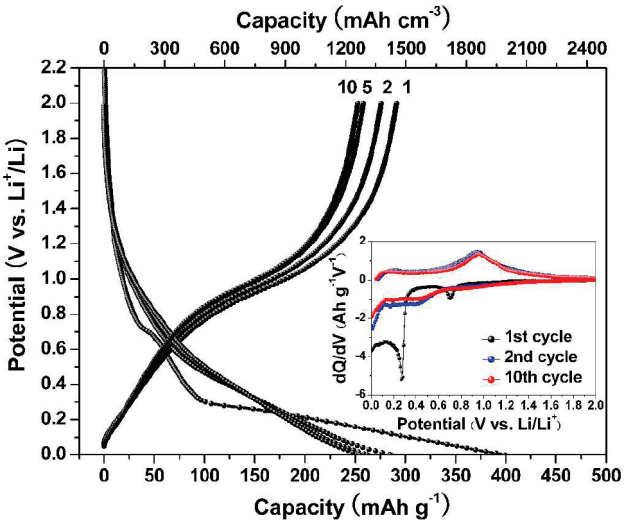

Figure 2. Electrochemical behavior of the VP electrode: (a) Voltage profile of the VP electrode for the 1st, 2nd, 5th, and 10th cycle. (b) DCP of the VP electrode for the for the 1st, 2nd, and 10th cycle.

nanocrystallites (Figure 1c). The crystallite size coincided with the above XRD results.

For an electrochemical evaluation of VP powder, electrodes were prepared by coating copper foil substrates with a slurry containing the active material (70 wt %), carbon black (Super P, 15 wt %) as a conducting agent and polyvinylidene fluoride (PVDF) dissolved in N-methyl pyrrolidinone (NMP) as a binder (15 wt %). Each component was mixed well to form a slurry, which was then coated onto a copper foil substrate followed by pressing and drying at 120 °C for 4 h under a vacuum. Laboratory-made coin-type electrochemical cells were assembled in an Ar-filled glovebox using Celgard 2400 as a separator, Li foil as the counter and reference electrodes, and 1 M $LiPF_6$ in ethylene carbonate (EC)/diethyl carbonate (DEC) (1:1 by volume, Samsung) as the electrolyte. All cells were tested galvanostatically between 0.0 and 2.0 V (vs. Li/Li^+) at a current density of 100 mA g^{-1} using a Maccor automated tester. Li was inserted into the electrode during discharging and extracted from the working electrode during charging.

Figure 2 shows the voltage profile and differential capacity plot (DCP) of the VP electrode. The first discharge and charge capacities of the VP electrode were 399 and 291 mA h g^{-1} (ca. 1990 and 1452 mAh cm^{-3}), respectively, with a Coulombic efficiency for the first cycle of 73%. Although the gravimetric capacity of the VP electrode is relatively small compared to that of graphite (372 mA h g^{-1}), its volumetric capacity was much higher than that of graphite (ca. 840 mA h cm^{-3}). Considering the first irreversible capacity from the conducting agent (Super P) used and SEI formation near 0.75 V,[29] it was concluded that approximately 1 mol of Li reacted with VP. Although the DCP shows a peak near 0.27 V during the first discharge, the DCP peaks from the first charge were similar.

(28) Suryanarayana, C. *Prog. Mater. Sci.* **2001**, *46*, 1.

(29) Peld, E. *J. Electrochem. Soc.* **1979**, *126*, 2047.

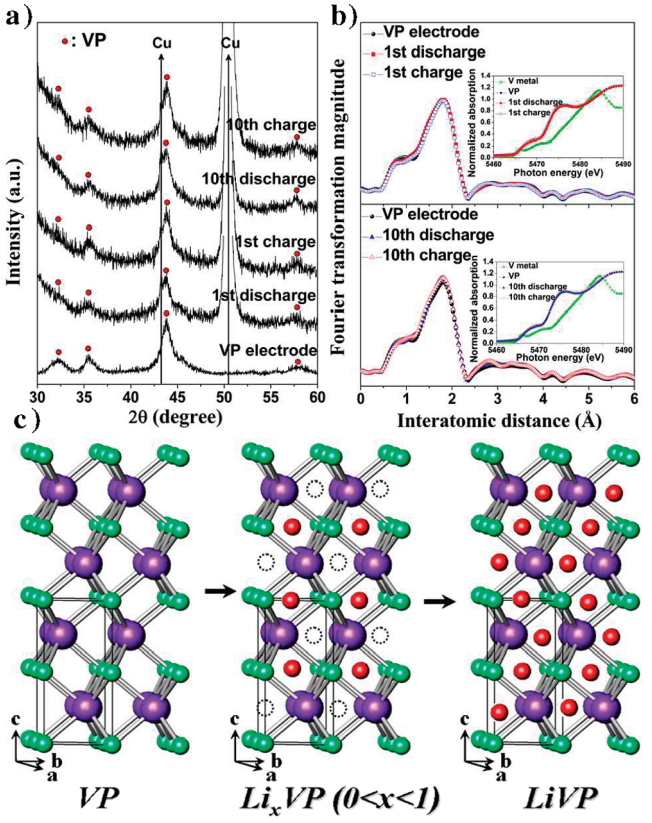

Figure 3. Reaction mechanism of the VP electrode: (a) Ex situ XRD patterns during the 1st and 10th cycle. (b) EXAFS and XANES results during the 1st and 10th cycle. (c) Suggested topotactic reaction mechanism of VP (V atoms, green; P atoms, purple; Li atoms, red).

Ex situ XRD analyses were carried out at the first and 10th cycles to confirm the electrochemical reaction mechanism of the VP electrode. As shown in Figure 3a, no structural changes during cycling were observed. X-ray absorption spectroscopy (XAS) analyses were performed to determine the structural changes occurring in the active material during cycling. The V K-edge spectra of the VP electrodes were recorded in transmission mode at the BL3C1 beamline (Electrochemistry, Pohang Light Source (PLS), Korea) in a storage ring of 2.5 GeV with a ring current of 120−170 mA. Figure 3b shows the V K-edge extended X-ray absorption fine structure (EXAFS) and X-ray absorption near edge structure (XANES, inset graph) spectra. At the first and 10th fully discharged and charged states, all peaks of EXAFS (2.8 Å, V−P bond distance; 3.2 Å, V−V bond distance) for the VP phase were almost the same as those of the pristine VP electrode. The V K-edge XANES spectra also shows no variation, which means that no V is produced and the redox process most likely occurs on the anion site, P or V−P bonds as suggested by Gillot et el.[30] The XANES result is similar to that of VP_2 electrode.[30] Ex situ XRD, EXAFS, and XANES demonstrated negligible structural changes in the hexagonal VP during Li insertion/extraction, which confirms the topotactic Li insertion/extraction in VP. The hexagonal VP structure has octahedral sites for Li accommodation and *a*-axis channels connected by each V and P atoms, which provides the voids and paths for Li insertion/extraction during the discharge/charge reactions without structural deterioration. Figure 3c shows a schematic diagram of the suggested mechanism of topotactic insertion/extraction of Li in VP based on ex situ XRD, EXAFS, XANES, and the crystal structure.

(30) Gillot, F.; Menetrier, M.; Bekaert, E.; Dupont, L.; Morcrette, M.; Monconduit, L.; Tarascon, J.-M. *J. Power Sources* **2007**, *172*, 877.

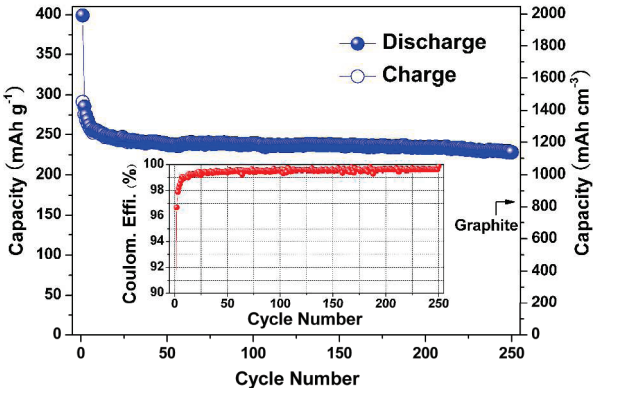

Figure 4. Cycle performance of the VP electrode between 0 and 2.0 V (vs Li/Li$^+$) at a cycling rate of 100 mA g^{-1} (inset graph: plot of the Coulombic efficiency vs cycle number).

Figure 4 presents the cycle performance and Coulombic efficiency of the VP electrode at a current of 100 mA g^{-1}. The cycle performance of the VP electrode was excellent. The VP electrode showed stable capacity of approximately 230 mA h g^{-1} or ca. 1150 mA h cm^{-3} over 250 cycles. In addition, a high Coulombic efficiency of ca. 99.5% was observed from the 20th cycle. Furthermore, the capacity retention of the discharge capacity of the first cycle was approximately 80% over 250 cycles. These high volumetric capacities and excellent cycle behavior were attributed to topotactic Li insertion/extraction in the VP electrode.

In conclusion, VP nanoparticles were prepared using a HEMM technique. When used as an anode material in rechargeable Li-ion batteries, the VP electrode showed high volumetric capacity (the first discharge and charge capacities corresponding to ca. 1990 and 1452 mAh cm^{-3}, respectively) and excellent cycling behavior (capacity retention of the discharge capacity of the first cycle of approximately 80% over 250 cycles). The excellent electrochemical behavior was attributed to topotactic Li insertion/extraction in the VP electrode. These exceptional electrochemical properties and topotactic concept highlight the potential of this VP as a new alternative anode material in Li-ion batteries.

Acknowledgment. The authors thank the Pohang Light Source (PLS) for the XAS measurements. This study was supported by the Korea Science and Engineering Foundation (KOSEF) through the Research Center for Energy Conversion and Storage at Seoul National University (Grant R11-2002-102-02001-0).